Title; Monocyte/macrophage-specific NADPH oxidase contributes to antimicrobial host defense in X-CGD.

Authors; Yuka Okura [1], Masafumi Yamada [1], Futoshi Kuribayashi [2], Ichiro Kobayashi [1], Tadashi Ariga [1]

[1] Department of Pediatrics, Hokkaido University Graduate School of Medicine, Sapporo, Japan

[2] Department of Biochemistry, Kawasaki Medical School, 577 Matsushima, Kurashiki, Japan

Correspondence to: Yuka Okura, Department of Pediatrics, Hokkaido University Graduate School of Medicine, North 15 West 7, Kita-ku, Sapporo, 060-8638, Japan

e-mail: okura@med.hokudai.ac.jp

Phone: +81-11-706-5954, Fax: +81-11-706-7898

Abstract

Background Chronic granulomatous disease (CGD) is a primary immunodeficiency disease that is characterized by susceptibility to bacterial and fungal infections. Various mutations in *CYBB* encoding the gp91^{phox} subunit of the phagocyte nicotinamide adenine dinucleotide phosphate (NADPH) oxidase impair the respiratory burst of all types of phagocytic cells and result in X-linked CGD (X-CGD).

Purpose We here sought to evaluate the underlying cause in an attenuated phenotype in an X-CGD patient. The patient is a 31-year-old male who had been diagnosed as having X-CGD based on the absence of nitroblue tetrazolium reduction and the presence of a *CYBB* mutation at the age of one year. He has been in good health after overcoming recurrent bacterial infections in infancy.

Methods We investigated genomic DNA analysis of *CYBB* gene, residual activity of NADPH oxidase, and expression of gp91^{phox} in both polymorphonuclear leukocytes (PMNs) and monocytes/macrophages in the present patient.

Results Although his underlying germline mutation, c.1016C>A (p.P339H) in the *CYBB* gene, was identified in both PMNs and monocytes, the expression and functional activity of gp91^{phox} retained in monocytes/macrophages, in stark contrast to markedly reduced PMNs.

Conclusions Our results indicate that residual reactive oxygen intermediates (ROI) production in PMNs plays an important role in infantile stage in X-CGD, but thereafter retained function of monocytes/macrophages might compensate for the function of NADPH oxidase deficient PMNs and might be an important parameter for predicting the prognosis of X-CGD patients.

Keywords:

X-linked chronic granulomatous disease; monocyte; macrophage; NADPH oxidase.

Introduction

Chronic granulomatous disease (CGD) is a primary immunodeficiency disorder characterized by recurrent life-threatening bacterial and fungal infections with granuloma formation. In addition, CGD is recognized as a hyperinflammatory condition [1]. Incidence of CGD is 1 in 200,000 to 250,000 live births [2], and the majority of the affected patients is diagnosed in infancy. Biochemically, CGD is characterized by abnormalities of one of the components of the nicotinamide adenine dinucleotide phosphate (NADPH) oxidase, resulting in the inability of phagocytic cells (neutrophils, eosinophils, monocytes, and macrophages) to generate reactive oxygen intermediates (ROI) which are needed for intracellular killing of phagocytized microorganisms. As for genetic abnormalities, more than two-thirds of CGD patients show X-linked recessive trait with mutations in the *CYBB* gene that encodes the $gp91^{phox}$, while the remaining patients have mutations in *CYBA*, *NCF-1*, *NCF-2*, and *NCF-4*, which encode $p22^{phox}$, $p47^{phox}$, $p67^{phox}$, and $p40^{phox}$ respectively and demonstrate autosomal recessive trait [3]. Generally, every phagocytic cell derived from X-CGD patients with germline mutation should show homogeneity for the expression of $gp91^{phox}$ and NADPH oxidase activity. Therefore, the functional diagnosis of CGD is usually based on the defective respiratory burst of PMNs as representative of leukocytes. Residual ROI production in neutrophils is known to be an important parameter for predicting clinical course and survival in CGD patients [4]. On the other hands, the effects of residual function in monocytes/macrophage lineage on clinical course in CGD patients are presently less clear. Herein, we report on an X-CGD patient carrying c.1016C>A (p.P339H) in the *CYBB* gene, yielding fair superoxide productive capability with near normal $gp91^{phox}$ expression in his monocytes/macrophages, in stark contrast to his PMNs.

Methods

The patient history

The patient is now a 31-year-old male who had a history of cervical suppurative lymphadenitis, stomatitis, otitis media, and skin abscess from 4 months to one year of age. He had been diagnosed as having X-CGD in his infancy by defective nitroblue tetrazolium reduction. The analysis of his family members demonstrated that his mother and his second sister were carriers, whereas his first oldest sister was not. Thereafter, he suffered from pneumonia and *Staphylococcal* skin infection following leg injury at the age of seven. He also suffered from protracted abdominal pain at the age of 20, but showed no abnormal findings and no granuloma formation on colonoscopy and histopathological examination. He had no history of apparent fungal infections, elevated serum β-D glucan levels, or excessive inflammatory condition including autoimmune disorders. He was currently in good health under prophylactic sulfamethoxazole/trimethoprim and itraconazole. His atypical clinical course described above prompted us to reevaluate his protective immunity.

Blood donors, cell preparations

Heparinized blood from the patient, his mother, his second oldest sister, four X-CGD patients, and healthy controls was obtained after informed consent according to the protocol approved by the Institutional Review Board of Hokkaido University Graduate School of Medicine. X-CGD1, 2, and 3 had c.1180_1182delinsATGTGATGAACACAT, IVS5 -3c>a, and c.161G>T (p.R54M) in the *CYBB* gene, respectively. X-CGD4 had 3.5 Mb deletion encompassing *XK*, *CYBB*, *RPGR*, and *OTC* in the X-chromosome gene [5]. X-CGD2 had a older bother who was diagnosed as having X-CGD with the

same causative mutation. Peripheral blood mononuclear cells (PBMC) were isolated by Ficoll-Hypaque density gradient centrifugation. After collecting the PBMC fraction, the cell pellet was collected and PMNs were obtained by using methylcellulose solution sedimentation and hypotonic lysis of contaminated erythrocytes. Monocytes were isolated from the positive fraction of PBMC using CD14 MicroBead (Miltenyi Biotec, Bergisch Gladbach, Germany) and MACS Separation Columns (Miltenyi Biotec) according to the manufacture's instructions. The purity of monocytes separated from PBMC was more than 96.0%, as determined by flow cytometry forward scatter/side scatter. Monocytes were resuspended in RPMI1640 supplemented with 10% fetal bovine serum (FBS) and penicillin/streptomycin. They were plated in 6-well plates at a density of 5×10^6 cells per well and then differentiated into macrophages by culturing for 10 days in the presence of 5 ng/ml of M-CSF (R&D Systems, Minneapolis, MN) at 37°C in humidified air containing 5% CO_2. Approximately 1/3 of the remaining medium was exchanged with newly prepared medium every 2-3 day.

Generation of EBV-transformed cell lines

EBV-transformed cell lines (EBV-LCLs) were generated by in vitro transformation of human B cells with EBV (strain B95-8), as described elsewhere [6].

DNA analysis

Genomic DNA was isolated from PMNs and monocytes by using SepaGene® (EIDIA, Ibaraki, Japan) according to the manufacture's instructions, and was analyzed for *CYBB* mutations by means of PCR amplification of each exon with its intronic boundaries, followed by sequence analysis.

Flow cytometric analysis of respiratory burst activity

Dihydrorhodamine 123 (DHR) is a conventionally used fluorescent probe for studying respiratory burst activity in PMNs [7]. This probe reacts with various ROI (*i.e.* superoxide, hydrogen peroxide, nitric oxide, and singlet oxygen) but was easily autoxidized by light. On the other hand, aminophenyl fluorescein (APF) [8] could evaluate ROI more reliably because this probe selectively detects highly reactive ROI such as hydroxyl radical and peroxynitrite and is resistant to autoxidation. In this study, we used these two probes, DHR (Molecular Probes) and APF (Sekisui Medicalm Tokyo, Japan), to more closely evaluate ROI production from monocytes as well as PMNs. Total leukocytes were isolated from 300 μL of blood with lysis buffer as previously described by Vowells et al [7]. Total leukocytes were washed in HBSS twice and activated for 15 min with phorbol myristate acetate (Sigma-Aldrich, St. Louis, MO), after incubation for 5 min at 37°C with DHR or APF in the presence of catalase (Sigma-Aldrich). The capacity of PMNs and monocytes to generate ROI was analyzed by flow cytometry using a FACSCalibur (BD, San Jose, CA). Fluorescence emitted by DHR and APF were detected by FL2 and FL1, respectively.

Flow cytometric analysis of surface expression of cytochrome b558

Surface cytochrome b558 expression was detected by flow cytometric analysis using monoclonal anti-gp91^{phox} antibody (7D5) (MBL, Nagoya, Japan). Total leucocytes and EBV-LCLs were washed in phosphate-buffered saline containing 1% FBS (PBS+FBS), blocked Fc receptor with 1:10 diluted healthy human serum for 5 min at room temperature, and reacted with 1:100 diluted anti-gp91^{phox} antibody or with 1:200 diluted mouse IgG1 (MOPC-21) (Sigma-Aldrich) for 30 min at 4°C. After being washed in PBS+FBS twice, they were reacted with 1:200 diluted fluorescein isothiocyanate-conjugated goat

anti-mouse IgG1 antibody (Southern Biotechnology Associates, Birmingham, AL) for 30 min at 4°C. Then, events of the PMNs and monocytes were analyzed by flow cytometry using FACSCalibur. Fluorescence intensity was detected by FL1.

Western blot analysis

To obtain whole-cell lysate, the cells were suspended with 200 μl of ice-cold PBS, in addition to 20 μl of 100% trichloroacetic acid and soon tapped and chilled for 20 min on ice. Lysates were then centrifuged at 15, 000 rpm for 20 min at 4°C. Supernatant fluids were discarded, and the remaining pellets were resuspended in 80 μl of UTM (9M urea, 2% Triton-X100, 5% 2-mercaptoethanol) and were disrupted by sonication. The particulate fraction was re-sonicated after adding 20 μl SDS solution (1.5% SDS, 0.2M Tris-Cl (pH 6.8), and appropriate bromophenol blue). Samples were separated by 10% polyacrylamide gels and transferred to Polyvinylidene fluoride membranes (Immobilon-P Transfer Membranes ; Merck Millipore, Billerica, MA). The membranes were blocked with 5% skim milk for 1 h at room temperature and were then incubated for two hours at room temperature with 1:3,000 diluted monoclonal mouse anti-gp91^{phox} antibody (BD). After three washes with Tris-buffered saline and 0.1% Tween 20 (TBS-T), membranes were incubated for two hours at room temperature with 1:2,000 diluted HRP-conjugated anti-mouse antibody (GE Healthcare, Buckinghamshire, U.K.). After three washes with TBS-T, the bands were visualized by Pierce Western blotting Substrate (Thermo, Rockford, IL). To control sample loading and protein transfer, the membrane was reprobed for 1:1,000 diluted β-actin (Sigma-Aldrich).

RT-PCR and quantitative RT-PCR analysis of CYBB

Total RNA was extracted with Trizol reagent (Invitrogen) from PMNs, monocytes, and EBV-LCL according to manufacture's protocols. First-strand cDNA was generated via transcription of 2 μg of total RNA using PrimeScript® RT Reagent Kit (Takara Bio, Otsu, Japan) in a total reaction volume of 40 μl according to the manufacture's instructions. RT-PCR was performed using the primers to amplify the coding exon 9 of *CYBB*: forward, 5'- TAGTGGGTCCCATGTTTCTGTATC-3'; reverse, 5'-ACATCACCACCTCATAGCTGAA-3'. RT-PCR products isolated by Gel-purification kit (Life Technologies Corporation, Carlsbad, CA) were then directly sequenced. Quantitative RT-PCR (qRT-PCR) was carried out on an ABI PRISM® 7000 (Applied Biosystems), using the SYBR Premix EX Taq™ II (Takara Bio). Control cDNA of the *CYBB* and *GAPDH* genes with five dilutions were used to obtain the standard curve, and then the PCR amplification efficiencies (E) for both genes was calculated according to the equation $E=10^{-1/slope} - 1$. The correlation coefficient (R^2) and slope values were obtained from the standard curve. Reactions were performed in a total volume of 25 μl volume containing 20 pg of cDNA template and 0.4 μM of each amplification primer. For *CYBB* the primers were: forward, 5'-GGCACTGAGGGTAGGTCTGACAA-3"; reverse, 5'-CAGTGTGAACAGGCTGGACCTAAG-3'. For *GAPDH* the primers were: forward, 5'-AATGACCCCTTCATTGACCTC-3'; reverse, 5'-ATGGGATTTCCATTGATGACA-3'. The PCR mixture was heat-denatured at 95°C for 30 s, followed by 40 cycles of 95°C for 5 s and 60°C for 31 s. As a control, PCR reaction mixtures without template cDNA were also analyzed in each assay. Each sample was tested in triplicate. Melting curves were calculated at the end of the cycles. The fluorescence threshold value (Ct value) was calculated using ABI PRISM® 7000 analysis software. The relative value of mRNA expression was calculated by the comparative ΔΔCt method. In brief, mean Ct values were normalized to the internal control GAPDH and the difference was defined as ΔCt. The

difference between the mean ΔCt values of compared samples was calculated and defined as ΔΔCt. The comparative mRNA expression level was expressed as $2^{-\Delta\Delta Ct}$. We used seven controls.

Results

Retained NADPH oxidase activity in monocytes

First of all, we studied respiratory burst activity of monocytes as well as PMNs by flow cytometry with DHR and APF to measure intracellular ROI production in the present patient, his mother, his second oldest sister, and three other X-CGD patients previously diagnosed. Respiratory burst activities measured by the mean fluorescence intensity (MFI) were shown in Table 1. The study with DHR demonstrated these three X-CGD patients almost completely lacked ROI in monocytes (the range of MFI; 0-5.44), despite the various ROI production from PMNs (the range of MFI; 0.35-76.47) (Fig. 1a). On the other hand, the present patient was shown to have significant ROI production in monocytes (MFI; 9.53), whereas he almost completely lacked ROI in PMNs (MFI; 2.51) (Fig. 1a). These findings were also confirmed by the analysis with APF (Fig. 1b). MFI by using APF revealed 6.92, 7.56, and 9.90 in PMNs and 37.94, 3.78, and 1.86 in monocytes, in the present patient, X-CGD2, and X-CGD3, respectively. These results indicate the present patient had retained functional activity of NADPH oxidase specifically in monocytes.

Retained $gp91^{phox}$ expression in monocytes

Next, we performed flow cytometric analysis of surface cytochrome b558 expression in PMNs and monocytes from the present patient, his mother, his second oldest sister, and the three X-CGD patients using anti-$gp91^{phox}$ antibody. The surface expression of cytochrome b558 was absent in both PMNs and monocytes from two classical X-CGD patients (X-CGD1 and X-CGD2), and was normal in both cells from a variant X-CGD patient (X-CGD3), indicating that surface expression of cytochrome

b558 is mostly concordant between PMNs and monocytes (Fig. 2a). On the other hand, surface expression of cytochrome b558 in the present patient was markedly reduced in PMNs, but was equivalent to control in monocytes (Fig. 2a). Then, to confirm total $gp91^{phox}$ expression in both PMNs and monocytes, we performed Western blot analysis of $gp91^{phox}$ (Fig. 3). The results showed that $gp91^{phox}$ in monocytes from the present patient was expressed equivalently to control, while the expression in PMNs was barely visible, which was consistent with the results of surface cytochrome b558 expression. The expression of $gp91^{phox}$ was absent in both cells from X-CGD1 and X-CGD2, while it was normal in both cells from X-CGD3.

Increased expression of gp65 in monocytes

The 65 kilodalton (kDa) intermediate, gp65, is the translation product of the *CYBB* gene, synthesized in the endoplasmic reticulum as a high-mannose precursor. The $gp65/p22^{phox}$ interaction is necessary for additional carbohydrate processing in the Golgi apparatus for the maturation gp65 into $gp91^{phox}$ [9-13] Bustamante *et al* has reported that macrophage-specific impairment of NADPH oxidase resulted in susceptibility to mycobacterial diseases in the patients carrying Q231P or T178P in the *CYBB* gene [14]. They assumed that increased expression of the gp65 in macrophages is associated with impaired formation of heterodimerization with $p22^{phox}$ as a cytochrome b_{558}, leading to impaired maturation of gp65 to $gp91^{phox}$. We detected 65 kDa bands which were immunoreactive with antibody specific for $gp91^{phox}$ in the monocyte samples (control, the present patient, and X-CGD3). The expression of gp65 was absent in X-CGD1 and X-CGD2, indicating that their mutations are critical for its biosynthesis. In the present patient and X-CGD3, normal $gp91^{phox}$ and increased gp65 expression compared with a control might suggest partial impairment of gp65 maturation into $gp91^{phox}$.

Shared *CYBB* mutation in both PMNs and monocytes

To elucidate the mechanism that caused different gp91^{phox} expression between PMNs and monocytes in the present patient, we performed genomic DNA analysis of *CYBB* gene in both cells for studying if there is somatic mosaicism. Only the substituted base of c.1016C>A was identified in both cells (Fig. 4), indicating retained expression and function of gp91^{phox} in monocytes were not attributable to somatic mosaicism.

Retained mRNA stability of the CYBB Pro339His mutant

We performed RT-PCR in both PMNs and monocytes from the present patient and his mother (Fig. 5a) and subsequent direct sequence analysis of the products (Fig. 5b). The results demonstrated that two signals of C and A in nucleotide 1016 were identified in both PMNs and monocytes from his mother. The amplitude of each signal seemed to be nearly the same in both cells, indicating that the stability of *CYBB* mRNA derived from the mutated allele was not different between the two cell populations. To further confirm this result, we carried out qRT-PCR analysis of the *CYBB* gene. No significant difference of gp91^{phox} mRNA was observed in PMNs and monocytes compared with control, respectively, suggesting that dichotomy of gp91^{phox} expression between PMNs and monocytes was not due to mRNA stability (Fig. 5c).

Retained cytochrome b558 expression in monocyte-derived macrophage

We also investigated surface expression of cytochrome b558 in monocyte-derived macrophages (MDMs) by flow cytometric analysis using anti-gp91^{phox} antibody, and found retained cytochrome b558

expression in MDMs derived from the present patient, as observed in monocytes (Fig. 2b). MDMs derived from X-CGD2 and X-CGD3 had absent and near normal cytochrome b558 expression, respectively. Thus, it was demonstrated that cytochrome b558 expression of MDMs is generally identical to that of monocytes.

Barely detectable gp91^{phox} expression in EBV-LCLs

We also studied gp91^{phox} expression in EBV-LCL, which are also known to express gp91^{phox}. We used X-CGD4 with total deletion of the *CYBB* gene as a negative control in the experiments. Western blot analysis demonstrated the expression of gp91^{phox} was barely detectable in EBV-LCL from the present patient, while that in X-CGD1, 2, and 4 was absent (Fig. 6a). We performed RT-PCR of EBV-LCLs cDNA for amplifying the *CYBB* fragment encompassing the c.1016C>A mutation and obtained the products from the present patient (Fig. 6b). No products were amplified in X-CGD4 as expected (Fig. 6b). To characterize the transcripts of the present patient, we performed subsequent sequence analysis of the products, demonstrating only the mutated signal of c.1016C>A (Fig. 6c). Flow cytometric analysis of the surface cytochrome b558 expression demonstrated a negative peak in EBV-LCL from the present patient, similar to that in X-CGD4 (Fig. 6d). X-CGD3 EBV-LCL also had a normal peak which is consistent with the results observed in PMNs and monocytes, indicating that cytochrome b558 might be expressed in approximately equal amounts regardless of the types of blood cells. Therefore, monocyte/macrophage-specific expression of gp91^{phox} in the present patient shows an unusual phenomenon.

Discussion

We demonstrated retained expression and function of gp91^{phox} specific to monocytes/macrophages from an adult X-CGD patient who showed an attenuated clinical presentation.

Mortality of CGD patients is high especially during the first two decades of life [15]. Invasive fungal infections, principally aspergillosis, increase with age and account for one-third to half of all deaths [2, 16-19]. CGD patients also frequently experience a variety of inflammatory complications such as granulomatous enteritis resembling Crohn's disease, and some have autoimmune disorders [20-23]. Although the present patient had suffered from recurrent bacterial infections during his first year of life, the incidence of infections decreased with age. He showed no histories of obvious fungal infections or subsequent uncontrollable granulomatous inflammation, which is distinct from the typical clinical course of X-CGD.

Neutrophils are front-line responders to invading pathogens. An essential function of NADPH oxidase-dependent ROI generation in neutrophils is microbial killing. Indeed, residual ROI production in neutrophils is known to be an important parameter for predicting favorable clinical course and survival of CGD [4]. On the other hands, the role of NADPH oxidase in monocytes/macrophages, both of which harbor gp91^{phox} expression, remains poorly understood. To our knowledge, X-CGD patients with retained function of NADPH oxidase specific to monocytes/macrophages as observed in the present patient have not been reported. There are, however, several studies of the engineered mice indicating the importance of monocyte/macrophage-specific NADPH oxidase activity for regulation of infections and hyperinflammation. Mice deficient for *Ncf1*, encoding p47^{phox} which is one component of the assembled NADPH oxidase complex, were used as murine models of CGD [24]. *Ncf1*-deficient mice

with transgenic rescue of *Ncf1* under the human CD68 promoter, which gained the expression of NCF1 and functional NADPH oxidase activity specifically in monocytes/macrophages, demonstrated that spontaneous or induced bacterial/fungal infections and the production of inflammatory cytokines in response to β-glucan were reduced compared with mice globally deficient for *Ncf1* [25-27]. Similarly, our results of the present patient suggest the specific contribution of monocyte/macrophage NADPH oxidase to antimicrobial host defense and to the downregulation of hyperinflammation which is often observed in an X-CGD patient with NADPH oxidase-incompetent phagocytic cells.

The underlying *CYBB* mutation of c.1016C>A (p.P339H) in the present patient was previously reported in 10 families of X-CGD patients [28-33] (http://structure.bmc.lu.se/idbase/) (Table 2). The patients from nine families were all classified into classical X-CGD. One of the patients, diagnosed as having X-CGD at the age of 3.5 years, required bone marrow transplantation following severe bacterial infections [32]. His ROI production of neutrophils measured by DHR assay revealed zero, while that of monocytes was not determined. Neutrophils from another patient were also revealed to have no production of ROI measured by DHR assay and 14-38% of normal surface $gp91^{phox}$ expression. Function or $gp91^{phox}$ expression of his monocytes was not assessed [30].

We demonstrated retained expression and function of $gp91^{phox}$ specifically in monocytes/macrophages from the present patient were not attributable to somatic mosaicism or retained mRNA stability in these cells (Fig. 4,5). As to cell-specific expression or function of $gp91^{phox}$, exactly the opposite phenomenon was reported by Bustamante *et al* [14]: macrophage-specific impairment of NADPH oxidase was demonstrated in patients carrying Q231P or T178P mutations in the *CYBB* gene who presented with susceptibility to mycobacterial diseases. The increased expression of gp65, the precursor of $gp91^{phox}$, in macrophages from these patients indicated impaired formation of the

heterodimer with $p22^{phox}$ as a cytochrome b_{558}, leading to maturational defects of gp65 into $gp91^{phox}$. Relatively higher expression of gp65 in monocytes from the present patient might suggest partially impaired maturation of gp65 into $gp91^{phox}$ in monocytes. We could not evaluate whether and how the impaired maturation is present in PMNs, since no gp65 expression was detectable in PMNs from the present patient and controls, which is possibly due to the instability of gp65 in PMNs [9, 14]. However, it is possible that $gp91^{phox}$ maturation is more severely impaired in PMNs than in monocytes in the present patient with undetermined mechanisms, which could have made the difference of $gp91^{phox}$ expression and function between these two cell populations.

It was not determined in this study whether the retained $gp91^{phox}$ expression and function specific to monocytes/macrophages is a phenomenon universal to patients with the P339H mutation, or unique to the present patient. In the former case, it is possible that there are more and more patients with the P339H mutation who were underdiagnosed because of the rarity of infection and that some patients manifested classical phenotypes with the contribution of environmental factors. In the latter case, some molecule(s) may have rescued the $gp91^{phox}$ maturation or stability to some extent specifically in the present patient's monocytes/macrophages with unknown mechanisms. Further investigation is needed to unravel the detailed mechanisms underlying the cell-specific impact of the germline mutation in PMNs, monocytes, and macrophages.

Conclusions

Our results provide a plausible mechanism to explain that NADPH oxidase in monocytes/macrophages plays an important role in both limiting microbial infection and downregulating inflammatory responses. It is also speculated that whereas residual neutrophil function is critical for innate immunity in infancy, monocyte/macrophage function could compensate for impaired neutrophil function with age. Assessments of monocytes as well as PMNs in X-CGD patients were needed, since residual NADPH oxidase in monocytes/macrophages might predict the long-term prognosis in X-CGD patients. Further characterization of cell-specific molecular mechanisms of bacterial and fungal clearance is important for elucidating the pathways involved in microbial defense and for the development of potential therapeutic targets for CGD.

Acknowledgements

M.Y., I.K., and T.A. contributed intellectually to the experimental process; F.K. kindly provided $gp91^{phox}$ antibody for flow cytometric analysis and Western blotting and intellectual guidance for the development of western blotting; Y.O. performed experiments and wrote the paper; and all authors commented on and discussed the paper. We thank the family members for participating in this work. This work was supported in part by a grant for Research on Intractable Diseases from the Japanese Ministry of Health, Labor and Welfare.

Conflicts of Interest Disclosures

The authors declare that they have no conflict of interest.

References

1. Schappi MG, Jaquet V, Belli DC, Krause KH. Hyperinflammation in chronic granulomatous disease and anti-inflammatory role of the phagocyte NADPH oxidase. Semin Immunopathol. 2008;30(3):255-71.
2. Winkelstein JA, Marino MC, Johnston RB, Jr., Boyle J, Curnutte J, Gallin JI, et al. Chronic granulomatous disease. Report on a national registry of 368 patients. Medicine (Baltimore). 2000;79(3):155-69.
3. Roos D, de Boer M. Molecular diagnosis of chronic granulomatous disease. Clin Exp Immunol. 2014;175(2):139-49.
4. Kuhns DB, Alvord WG, Heller T, Feld JJ, Pike KM, Marciano BE, et al. Residual NADPH oxidase and survival in chronic granulomatous disease. N Engl J Med. 2010;363(27):2600-10.
5. Yamada M, Arai T, Oishi T, Hatano N, Kobayashi I, Kubota M, et al. Determination of the deletion breakpoints in two patients with contiguous gene syndrome encompassing CYBB gene. Eur J Med Genet. 2010;53(6):383-8.
6. Tosato G, Cohen JI. Generation of Epstein-Barr Virus (EBV)-immortalized B cell lines. Curr Protoc Immunol. 2007;Chapter 7:Unit 7 22.
7. Vowells SJ, Sekhsaria S, Malech HL, Shalit M, Fleisher TA. Flow cytometric analysis of the granulocyte respiratory burst: a comparison study of fluorescent probes. J Immunol Methods. 1995;178(1):89-97.
8. Setsukinai K, Urano Y, Kakinuma K, Majima HJ, Nagano T. Development of novel fluorescence probes that can reliably detect reactive oxygen species and distinguish specific species. J Biol

Chem. 2003;278(5):3170-5.

9. Porter CD, Parkar MH, Verhoeven AJ, Levinsky RJ, Collins MK, Kinnon C. p22-phox-deficient chronic granulomatous disease: reconstitution by retrovirus-mediated expression and identification of a biosynthetic intermediate of gp91-phox. Blood. 1994;84(8):2767-75.

10. Porter CD, Kuribayashi F, Parkar MH, Roos D, Kinnon C. Detection of gp91-phox precursor protein in B-cell lines from patients with X-linked chronic granulomatous disease as an indicator for mutations impairing cytochrome b558 biosynthesis. Biochem J. 1996;315:571-5.

11. Yu L, Zhen L, Dinauer MC. Biosynthesis of the phagocyte NADPH oxidase cytochrome b558. Role of heme incorporation and heterodimer formation in maturation and stability of gp91phox and p22phox subunits. J Biol Chem. 1997;272(43):27288-94.

12. Yu L, DeLeo FR, Biberstine-Kinkade KJ, Renee J, Nauseef WM, Dinauer MC. Biosynthesis of flavocytochrome b558 . gp91(phox) is synthesized as a 65-kDa precursor (p65) in the endoplasmic reticulum. J Biol Chem. 1999;274(7):4364-9.

13. DeLeo FR, Burritt JB, Yu L, Jesaitis AJ, Dinauer MC, Nauseef WM. Processing and maturation of flavocytochrome b558 include incorporation of heme as a prerequisite for heterodimer assembly. J Biol Chem. 2000;275(18):13986-93.

14. Bustamante J, Arias AA, Vogt G, Picard C, Galicia LB, Prando C, et al. Germline CYBB mutations that selectively affect macrophages in kindreds with X-linked predisposition to tuberculous mycobacterial disease. Nat Immunol. 2011;12(3):213-21.

15. Finn A, Hadzic N, Morgan G, Strobel S, Levinsky RJ. Prognosis of chronic granulomatous disease. Arch Dis Child. 1990;65(9):942-5.

16. Jones LB, McGrogan P, Flood TJ, Gennery AR, Morton L, Thrasher A, et al. Chronic

granulomatous disease in the United Kingdom and Ireland: a comprehensive national patient-based registry. Clin Exp Immunol. 2008;152(2):211-8.

17. Kobayashi S, Murayama S, Takanashi S, Takahashi K, Miyatsuka S, Fujita T, et al. Clinical features and prognoses of 23 patients with chronic granulomatous disease followed for 21 years by a single hospital in Japan. Eur J Pediatr. 2008;167(12):1389-94.

18. van den Berg JM, van Koppen E, Ahlin A, Belohradsky BH, Bernatowska E, Corbeel L, et al. Chronic granulomatous disease: the European experience. PLoS One. 2009;4(4):e5234.

19. Ahlin A, Fugelang J, de Boer M, Ringden O, Fasth A, Winiarski J. Chronic granulomatous disease-haematopoietic stem cell transplantation versus conventional treatment. Acta Paediatr. 2013;102(11):1087-94.

20. Sanford AN, Suriano AR, Herche D, Dietzmann K, Sullivan KE. Abnormal apoptosis in chronic granulomatous disease and autoantibody production characteristic of lupus. Rheumatology (Oxford). 2006;45(2):178-81.

21. Rosenzweig SD. Inflammatory manifestations in chronic granulomatous disease (CGD). J Clin Immunol. 2008;28 Suppl 1:S67-72.

22. De Ravin SS, Naumann N, Cowen EW, Friend J, Hilligoss D, Marquesen M, et al. Chronic granulomatous disease as a risk factor for autoimmune disease. J Allergy Clin Immunol. 2008;122(6):1097-103.

23. Marks DJ, Miyagi K, Rahman FZ, Novelli M, Bloom SL, Segal AW. Inflammatory bowel disease in CGD reproduces the clinicopathological features of Crohn's disease. Am J Gastroenterol. 2009;104(1):117-24.

24. Jackson SH, Gallin JI, Holland SM. The p47phox mouse knock-out model of chronic

granulomatous disease. J Exp Med. 1995;182(3):751-8.

25. Pizzolla A, Hultqvist M, Nilson B, Grimm MJ, Eneljung T, Jonsson IM, et al. Reactive oxygen species produced by the NADPH oxidase 2 complex in monocytes protect mice from bacterial infections. J Immunol. 2012;188(10):5003-11.

26. Deffert C, Carnesecchi S, Yuan H, Rougemont AL, Kelkka T, Holmdahl R, et al. Hyperinflammation of chronic granulomatous disease is abolished by NOX2 reconstitution in macrophages and dendritic cells. J Pathol. 2012;228(3):341-50.

27. Grimm MJ, Vethanayagam RR, Almyroudis NG, Dennis CG, Khan AN, D'Auria AC, et al. Monocyte- and macrophage-targeted NADPH oxidase mediates antifungal host defense and regulation of acute inflammation in mice. J Immunol. 2013;190(8):4175-84.

28. Liese JG, Jendrossek V, Jansson A, Petropoulou T, Kloos S, Gahr M, et al. Chronic granulomatous disease in adults. Lancet. 1996;347(8996):220-3.

29. Rae J, Newburger PE, Dinauer MC, Noack D, Hopkins PJ, Kuruto R, et al. X-Linked chronic granulomatous disease: mutations in the CYBB gene encoding the gp91-phox component of respiratory-burst oxidase. Am J Hum Genet. 1998;62(6):1320-31.

30. Roesler J, Heyden S, Burdelski M, Schafer H, Kreth HW, Lehmann R, et al. Uncommon missense and splice mutations and resulting biochemical phenotypes in German patients with X-linked chronic granulomatous disease. Exp Hematol. 1999;27(3):505-11.

31. Heyworth PG, Curnutte JT, Rae J, Noack D, Roos D, van Koppen E, et al. Hematologically important mutations: X-linked chronic granulomatous disease (second update). Blood Cells Mol Dis. 2001;27(1):16-26.

32. Wolach B, Gavrieli R, de Boer M, Gottesman G, Ben-Ari J, Rottem M, et al. Chronic

granulomatous disease in Israel: clinical, functional and molecular studies of 38 patients. Clin Immunol. 2008;129(1):103-14.

33. Roos D, Kuhns DB, Maddalena A, Roesler J, Lopez JA, Ariga T, et al. Hematologically important mutations: X-linked chronic granulomatous disease (third update). Blood Cells Mol Dis. 2010;45(3):246-65.

Table 1 Respiratory burst activities measured as mean fluorescence intensity in PMNs and Mono

	DHR		APF	
	PMNs	Mono	PMNs	Mono
Control	353.92	70.47	1101.66	267.62
Patient	2.51	9.53	6.92	37.94
X-CGD1	0.35	0	N.D.	N.D.
X-CGD2	28.12	5.44	7.56	3.78
X-CGD3	76.47	4.24	9.90	1.86

N.D. not determined

Table 2 X-CGD patients with p.P339H mutation

Family	Age at diagnosis	Classification by ROI production	Clinical manifestation	Reference
The present case	one year old	PMNs : markedly reduced Mono ; retained	An attenuated phenotype	
1	N.D.	Classical X-CGD	Severe illness	[29]
2	N.D.	Classical X-CGD	N.D.	[28, 30]
3	N.D.	N.D.	N.D.	[31]
4*	N.D.	Classical X-CGD	N.D.	[33]
5*	N.D.	Classical X-CGD	N.D.	[33]
6	N.D.	Classical X-CGD	N.D.	[33]
7	N.D.	Classical X-CGD	N.D.	[33]
8	N.D.	Classical X-CGD	N.D.	[33]
9	N.D.	Classical X-CGD	N.D.	[33]
10	3.5 years old	Classical X-CGD	Severe illness, BMT	[32, 33]

ROI reactive oxygen intermediates, *N.D.* not determined, *BMT* bone marrow transplantation

4*, 5* : The patients had another classical X-CGD patient in their relatives.

Figure Legends

Fig. 1 Intracellular ROI production of PMNs was substantially reduced, while that of monocytes was fairly retained in the present patient. Flow cytometric analysis of ROI production in PMA-stimulated PMNs and monocytes using DHR (a) or APF (b) as fluorescent probes. Shaded area, unstimulated cells; open area, stimulated cells. APF assays from X-CGD1, his mother, and his sister were not performed. *ROI* reactive oxygen intermediates, *PMA* phorbol myristate acetate, *PMNs* Polymorphonuclear leukocytes, *Mono* monocytes, *DHR* dihydrorhodamine 123, *APF* aminophenyl fluorescein

Fig. 2 Surface cytochrome b558 expression was markedly reduced in PMNs, but equivalent to control in monocytes and MDMs in the present patient. Flow cytometric analysis of surface cytochrome b558 expression in PMNs (a), monocytes (a), and monocyte-derived macrophages (MDMs) (b). Shaded area, negative control cells reacted with mouse IgG1; open area, cells reacted with anti-gp91^{phox} antibody. MDMs assays derived from X-CGD1 and his mother were not performed. *MDMs* monocyte-derived macrophages

Fig. 3 Monocyte-specific expression of gp91^{phox} in the present patient was observed by Western blotting. Western blotting analysis of gp91^{phox} expression in whole cell lysates from PMNs and monocytes. PMNs and monocytes from a control, X-CGD patients (X-CGD1, X-CGD2, X-CGD3), and the present patient were probed with an antibody against gp91^{phox} and an antibody against actin (loading control). Left magin, molecular size in kDa

Fig. 4 The c.1016C>A mutation in the *CYBB* gene was shared by both PMNs and monocytes from the present patient. Direct sequence analysis of *CYBB* exon 9 in PMNs and monocytes from the present patient. The results of his sister and a control were also shown. Forward sequence was shown

Fig. 5 Retained mRNA stability of the *CYBB* P339H mutant. (a) RT-PCR analysis of *CYBB* and *GAPDH* in PMNs and monocytes derived from control, the present patient, and his mother and a water sample. (b) Direct sequence analysis of the *CYBB* RT-PCR products in the present patient and his mother. Forward and reverse sequences were shown. (c) Quantitative RT-PCR of $gp91^{phox}$ in PMNs and monocytes. The line across the box indicates the median. The box indicates the 25th and 75th percentiles. Whiskers represent the maximum and minimum values

Fig. 6 The $gp91^{phox}$ expression in EBV-LCL was barely detectable by Western blotting and not detected by flow cytometric analysis using an anti-$gp91^{phox}$ antibody in the present patient. (a) Western blot analysis of $gp91^{phox}$ expression in EBV-LCL. (b) RT-PCR analysis of *CYBB* in EBV-LCLs. (c) Direct sequence analysis of the products. Forward sequence was shown. (d) Flow cytometric analysis of surface cytochrome b558 expression in EBV-LCL using an anti-$gp91^{phox}$ antibody

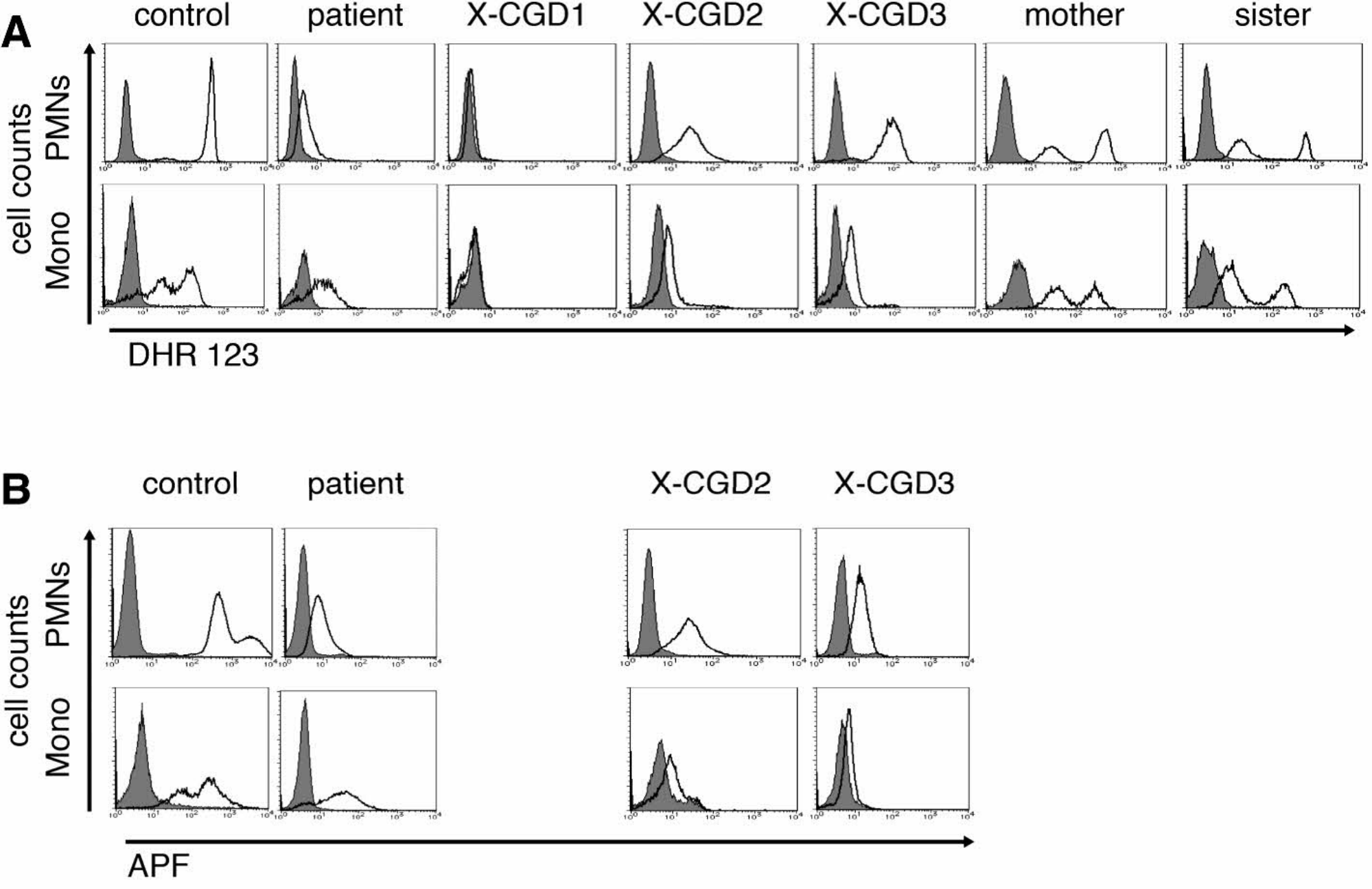
A
control
patient
X-CGD1
X-CGD2
X-CGD3
mother
sister
cell counts
PMNs
Mono
DHR 123
B
control
patient
X-CGD2
X-CGD3
cell counts
PMNs
Mono
APF

Figure 1

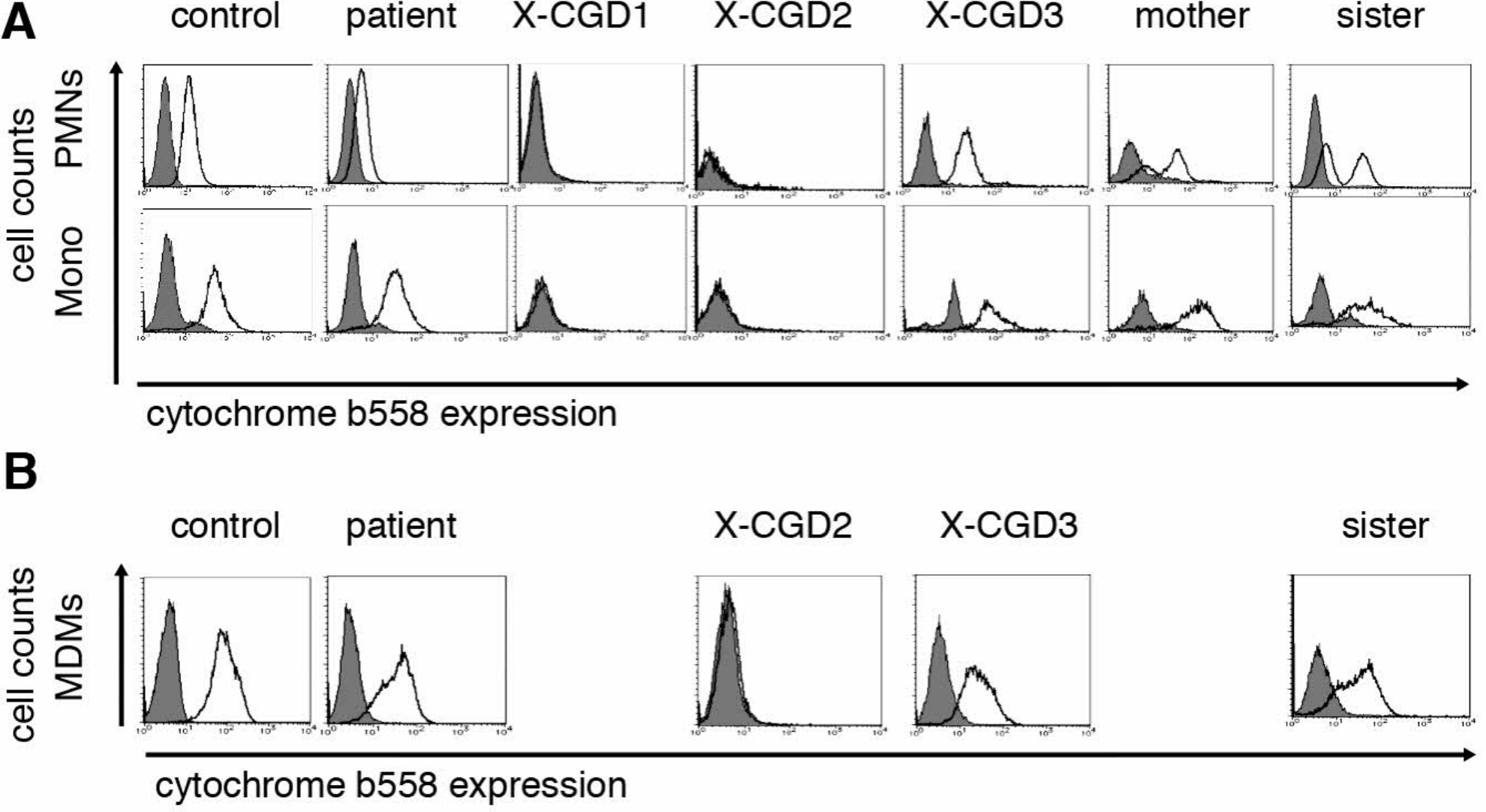
A
control
patient
X-CGD1
X-CGD2
X-CGD3
mother
sister
cell counts
PMNs
Mono
cytochrome b558 expression
B
control
patient
X-CGD2
X-CGD3
sister
cell counts
MDMs
cytochrome b558 expression

Figure 2

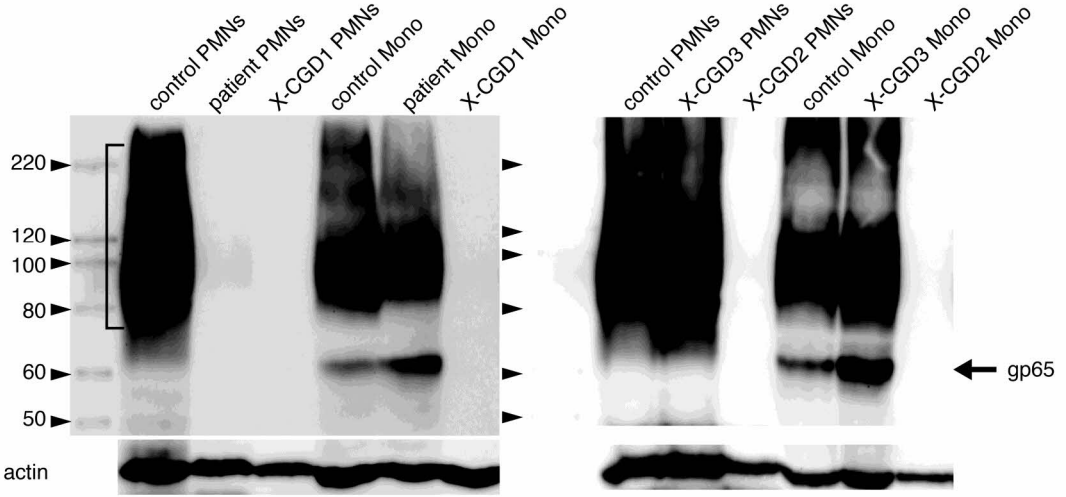
control PMNs
patient PMNs
X-CGD1 PMNs
control Mono
patient Mono
X-CGD1 Mono
control PMNs
X-CGD3 PMNs
X-CGD2 PMNs
control Mono
X-CGD3 Mono
X-CGD2 Mono
220
120
100
80
60
50
actin
gp65

Figure 3

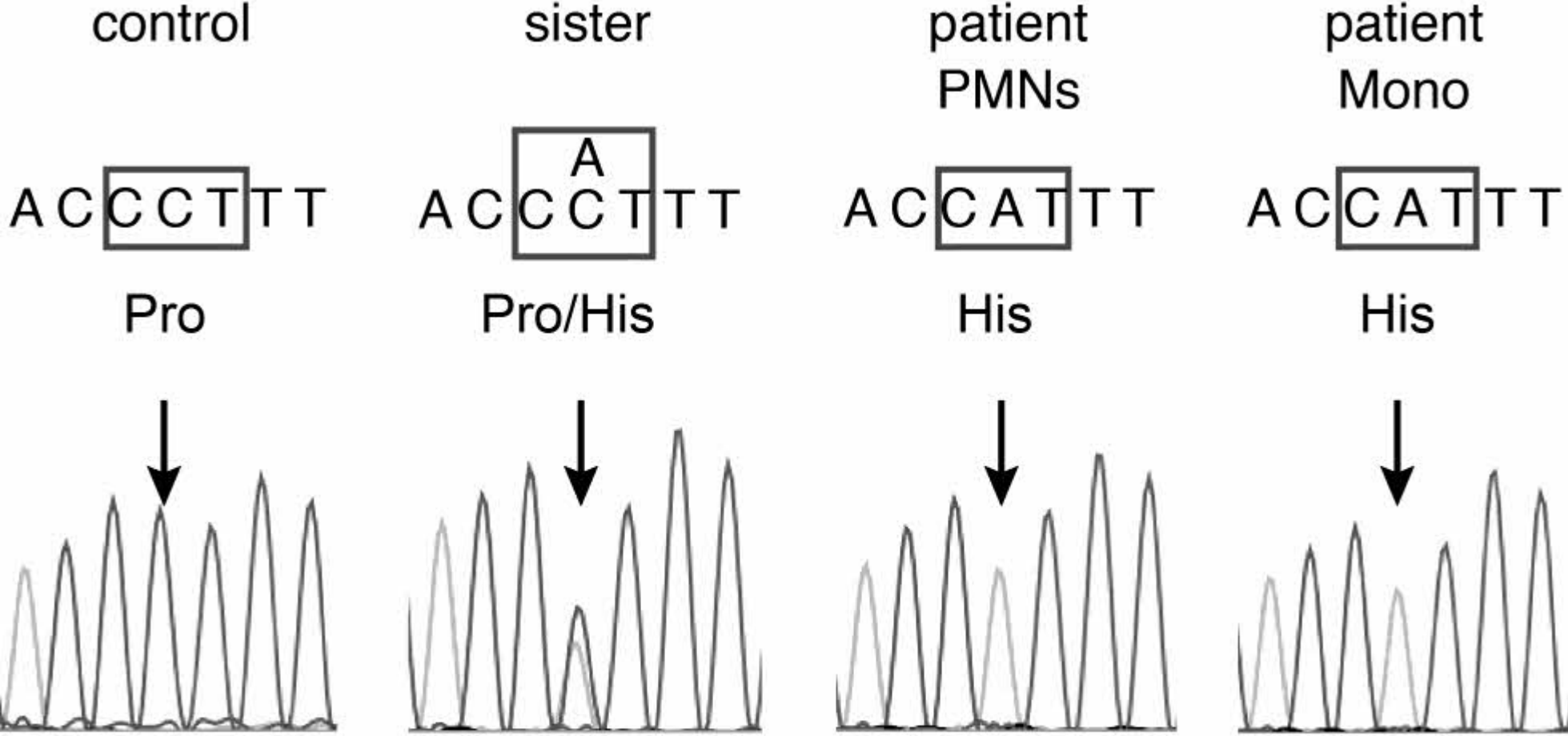
control
sister
patient PMNs
patient Mono
A C C C T T T
A
A C C C T T T
A C C A T T T
A C C A T T T
Pro
Pro/His
His
His

Figure 4

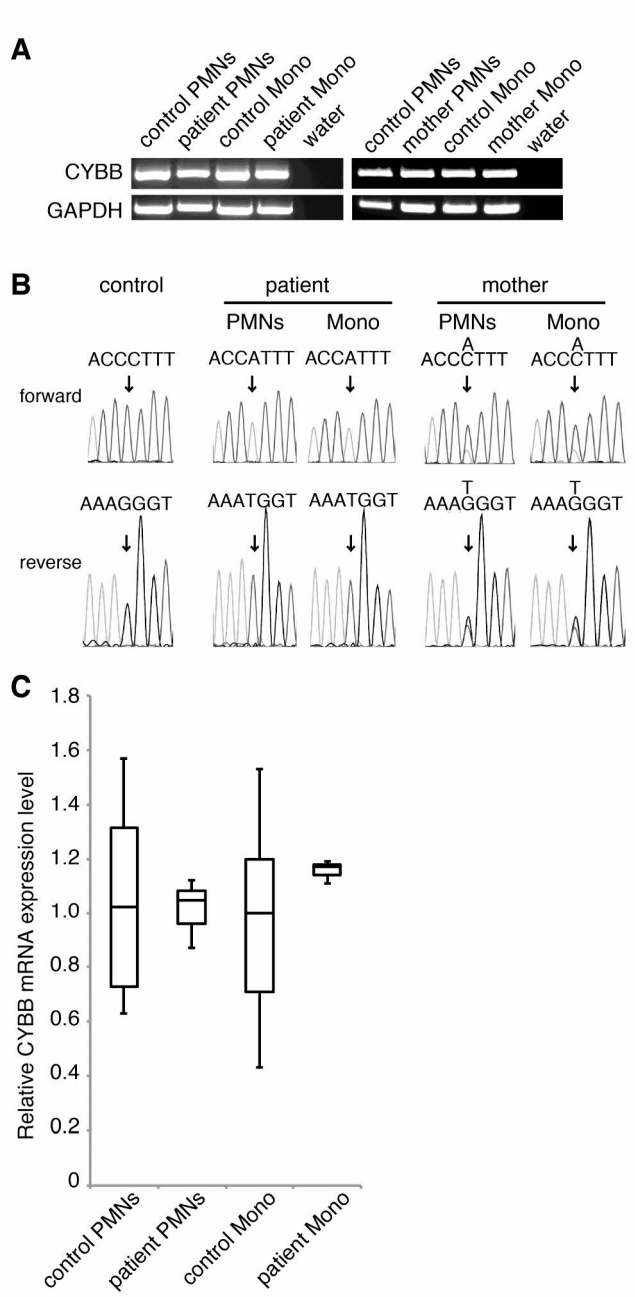
A
control PMNs
patient PMNs
control Mono
patient Mono
water
control PMNs
mother PMNs
control Mono
mother Mono
water
CYBB
GAPDH
B
control
patient
mother
PMNs
Mono
PMNs
Mono
ACCCTTT
ACCATTT
ACCATTT
ACCCTTT
ACCCTTT
A
A
forward
AAAGGGT
AAATGGT
AAATGGT
AAAGGGT
AAAGGGT
T
T
reverse
C
Relative CYBB mRNA expression level
1.8
1.6
1.4
1.2
1.0
0.8
0.6
0.4
0.2
0
control PMNs
patient PMNs
control Mono
patient Mono

Figure 5

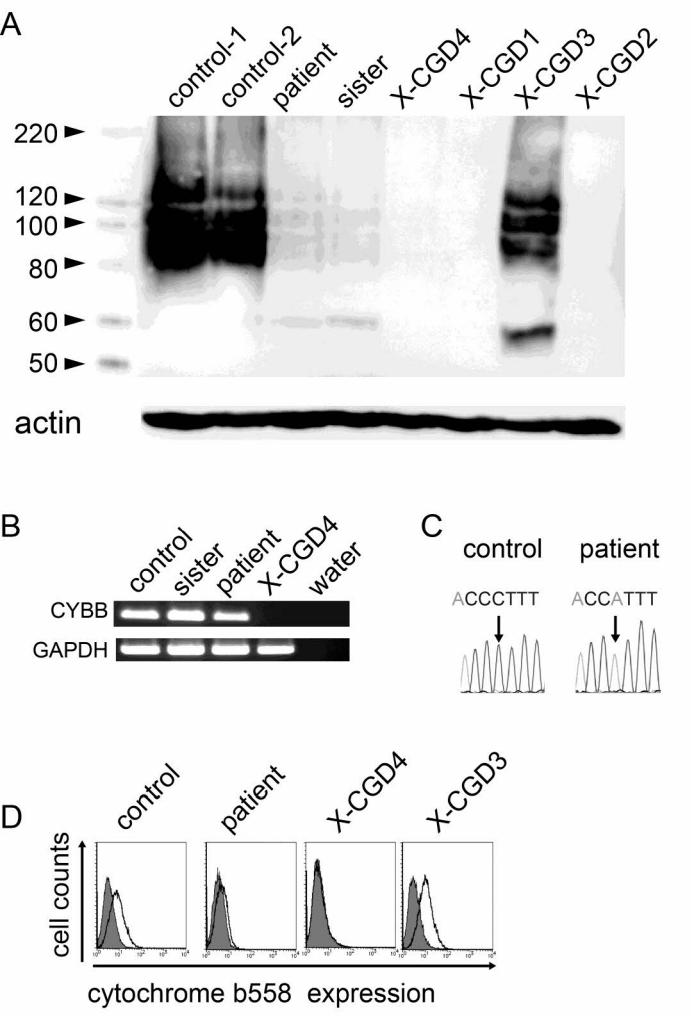
A
control-1
control-2
patient
sister
X-CGD4
X-CGD1
X-CGD3
X-CGD2
220
120
100
80
60
50
actin
B
control
sister
patient
X-CGD4
water
CYBB
GAPDH
C
control
patient
ACCCTTT
ACCATTT
D
control
patient
X-CGD4
X-CGD3
cell counts
cytochrome b558 expression

Figure 6